ANNALS OF FACULTY ENGINEERING HUNEDOARA
- INTERNATIONAL JOURNAL OF ENGINEERING
Tome IX (Year 2011). Fascicule 2. (ISSN 1584 - 2665)

[1.]Paolo BOSCARIOL, [2.]Alessandro GASPARETTO,
[3.]Albano LANZUTTI, [4.]Renato VIDONI, [5.]Vanni ZANOTTO

NEUMESY: A SPECIAL ROBOT FOR NEUROSURGERY

[1-5.] UNIVERSITY OF UDINE – DIEGM. VIA DELLE SCIENZE 208, 33100 UDINE, ITALY

ABSTRACT: In the last years a large number of new surgical devices have been developed so as to improve the operation outcomes and reduce the patient's trauma. Nevertheless the dexterity and accuracy required in positioning the surgical devices are often unreachable if the surgeons are not assisted by a suitable system. From a kinematic point of view, the robot must reach any target position in the patient's body being less invasive as possible with respect to the surgeon's workspace. In order to meet such requirements a suitable design of the robot kinematics is needed. This paper presents the kinematic design of a special robot for neurosurgical operations, named NEUMESY (NEUrosurgical MEchatronic SYstem).
NEUMESY is a six joints serial manipulator whose kinematic structure lets the robot to adapt to different patient's positions while minimizing the overall dimensions. Owing to the usual symmetry of a surgical tool, the kinematic dimension of the neurosurgical task is five, being given by one point and one direction on the space. Therefore the NEUMESY is kinematically redundant, leaving an extra DOF to the surgeon to choose a suitable robot configuration which minimally limits his movements during the surgical operations. The link lengths have been optimized in order to maximize the robot workspace with respect to the surgical task, while minimizing the links static deformations.
KEYWORDS: surgical devices, kinematic design, special robot, neurosurgical operations, NEUMESY

❖ INTRODUCTION

The initial experimentation of robotic systems in surgery was undertaken during the early 1980s [6,7,3], and it basically consisted of adapting the industrial robot technologies already in existence. In the last decade, there has been a growing awareness, within the medical community, of the benefits offered by using robots in various surgical tasks. Traditional surgery involves making large incisions to access the part of a patient's body that needs to be operated on. Minimally Invasive Surgery (MIS), on the other hand, is a cost-effective alternative to open surgery. Basically, the same operations are performed using instruments designed to enter the body cavity through several tiny incisions, rather than a single large one. By eliminating large incisions, trauma to the body, post-operative pain, and the length of hospital stay are significantly reduced.

However, new problems connected to the use of robots in surgery have arisen, since there is no direct contact with the patient. For this reason, it is necessary to develop suitable tactile sensors to provide surgeons with the perception of directly operating on the patient. Such a result can be achieved by using force feedback systems, in which the force applied to patient's tissue is fed back to a robotic device (haptic master) directly operated by the surgeon.

We can categorize surgical robots based on their different roles during surgical treatment [4,5] Passive robots only serve as a tool-holding device once directed to the desired position. Semi-active devices perform the operation under direct human control. Active devices are under computer control and automatically perform certain interventions. Moreover, the surgical robot can have different levels of autonomy. To be specific, systems that are able to perform fully automated procedures are called autonomous. On the other hand, when the surgeon completely controls every single motion of the robot, this is called a tele-operated system or a master-slave system. Medical robotics has found fruitful ground especially in neurosurgical applications, owing to the accuracy required by the high functional density of the central nervous system [6,11,9].

In past decades, several different robotic neurosurgical devices have been created. A comprehensive survey can be found in [4]. In particular, in the 1980s Benabid and colleagues [1,2] experimented with an early precursor to the robot marketed as Neuromate [5] (Renishaw Mayfield, UK).

© copyright FACULTY of ENGINEERING - HUNEDOARA, ROMANIA

Today's robot projects focus on three major areas of improvement [4]:

- ❖ increasing the overall accuracy of the classical stereotactic systems
- ❖ increasing the added-value of the equipment
- ❖ enhancing the capabilities of the surgeon

The Mechatronics Research Group (composed of researches of the University of Padova, University of Udine and University of Trieste, Italy) [10] with the assistance of the Neurosurgical Department of the University of Florence [11] has developed two master-slave robotic systems for minimally-invasive neurosurgical operations. The first robot (Figure 1), named LANS (Linear Actuator for Neuro Surgery) has been conceived specifically to perform biopsies and neurosurgical interventions by means of a miniaturized x-ray source (the PRS, Photon Radiosurgery System, by Carl Zeiss), whose emitting tip must be placed accurately inside the patient's brain tissues [12,13]. The LANS robotic system is composed of a haptic master module, operated by the surgeon, and a slave mechatronic module moving a PRS probe, or a biopsy needle, along a predefined emission axis in accordance with the master position imposed by the surgeon. In order to orient the LANS along the established emission axis, a NeuroMate robot is employed in a frame-based configuration which ensures the highest possible accuracy. The system has been designed assuming that during the surgical operation only the LANS (which is very accurate, and provides the surgeon with force feedback) is in active mode while the NeuroMate is powered off. This allows overcoming much of the problems associated with the complex nature of this surgical therapy. Moreover, very precise and repeatable movements of the biopsy needle and of the x-ray source can be obtained, thus improving the overall intervention outcomes.

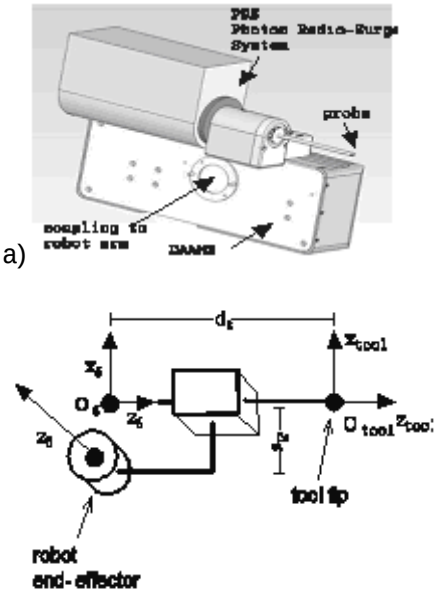

Fig. 1 (a) The DAANS actuator and the PRS *x*-ray source (b) Simplified kinematic structure of the DAANS

DAANS (Double Action Actuator for NeuroSurgery, [14]) is the second robot (Figure 1) carried out by Mechatronics research group. The aim of the system is to provide another degree of freedom to the PRS source about the emission axis. The system allows extending the therapy with PRS also to irregular shape tumorous lesions, by integrating translation and spin movements of the source. Indeed, single isocenter radiosurgery procedures produce nearly spherical isodose distributions. In order to avoid unacceptable dose delivery to non target tissues, the high-dose region must be shaped to fit individual targets. The high-dose region can be manipulated into a variety of shapes that closely conform to a tumour shape by means of shielding caps and multiple targets dose delivery. The caps are placed on the probe of the x-ray source as in Figure 4(a). Nevertheless, LANS and DAANS limit the NeuroMate mobility, owing to their geometrical dimension, which can interfere with the robot arm movements (Figure 2(b)). In this manner the NeuroMate workspace is reduced and some tool configuration is not reachable [12-14]. This paper presents the results of a preliminary analysis on the kinematic structure of a new surgical robot, named NEUMESY. The robot is able to maximize the performances of the therapy by means of the DAANS and PRS, increasing the workspace of the overall robotic system and allowing all possible tool configurations on the patient's head to be reached.

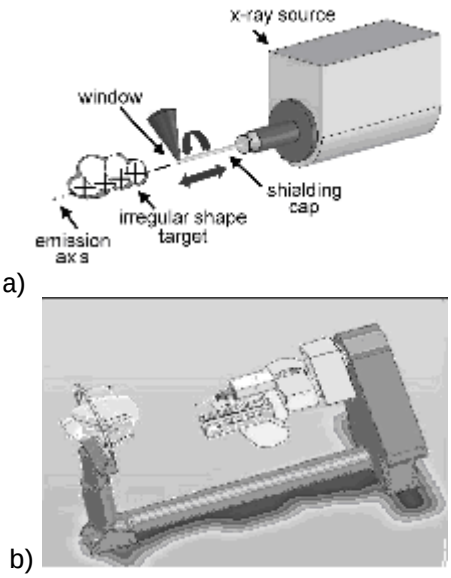

Figure 2: (a) PRS and shielding caps (b) NEUROMATE and DAANS

❖ THE STUDY

Introducing a robot in an operating room must fulfill some elementary rules. From a kinematics point of view two types of constraints can be taken: medical requirements and robotics requirements [15].

Medical requirements

For sterilization reasons no non-medical equipment must be closer than a fixed distance from the operating site. Thus the robot must collide neither with the patient, nor with the medical staff, nor with the surgical tools [15].

The requirement becomes quite complex in the frame-based applications, where the stereotactic frame (the mechanical structure the patient's head is fixed on) interferes with the robot movements. In order to satisfy this requirement, it is useful to define a virtual sphere (Figure 3) including the patient's head and the stereotactic frame. The robot must neither cross nor touch this sphere. The radius of the sphere depends on the stereotactic frame dimensions, while the center is on the patient's head. Moreover, the robot must minimally limit the surgeon's movements during the operation. To this end, the surgeon must be able to choose a suitable robot configuration for each tool position and the robot must adapt its workspace to the surgeon's requirements, which may change during the surgical task.

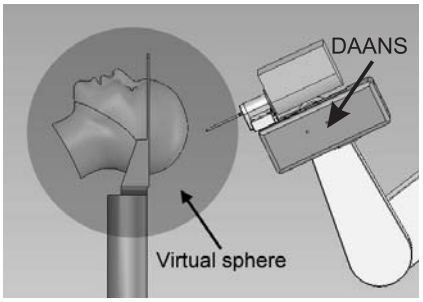

Figure 3. The virtual sphere includes the patient's head and the stereotactic frame

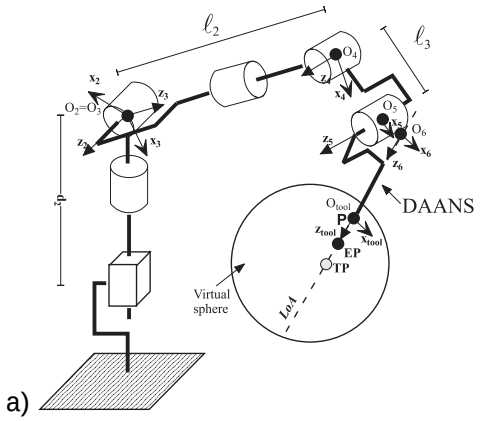

a)

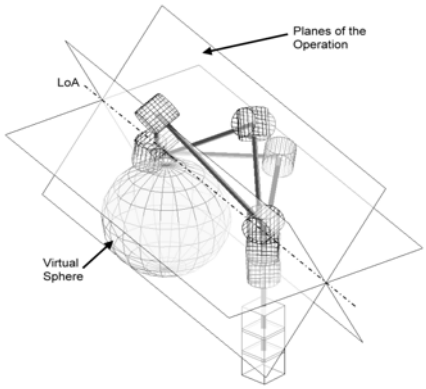

b)

Figure 4 (a) The NEUMESY, the DAANS and the virtual sphere (b) Three robot configurations for the same TP and LoA

Robotics requirements

The robotics constraints concern the structure of the NEUMESY in order to satisfy the above medical constraints. The preliminary choice considers the robot kinematic structure. The advantages of a serial robot if compared to a parallel one are due to the larger workspace and the higher dexterity and manipulability. On the other hand a parallel manipulator is stiffer allowing higher accuracy in the tool positioning. According to the medical constraints, the robot has to be able to avoid the virtual sphere and it must minimally limit the surgeon's movements. Therefore, the solution adopted consists in a serial structure.

Nevertheless this choice requires a links length optimization so as to maximize both the workspace and the stiffness of the robot.

Moreover, since the neurosurgical tools have usually an axial symmetry, only two spatial points on the patient's head have to be stated by the surgeons. The first one is the Target Point (TP), the center of the cerebral lesion where the tool has to be placed, while the second one is the Entry Point (EP), the hole through which the surgical instruments go into the skull. EP and TP state the Line of Action (LoA) along which the tools should be moved (Figure 4). Since the surgical operation fixes only five constraints on the space, a five DoF manipulator should be sufficient to a neurosurgical operation, nevertheless, a further DOF yields the kinematic redundancy which allows infinite configuration for the same surgical task, letting the surgeon choose the suitable one.

❖ ANALISES, DISCUSIONS, APPROACHES AND INTERPRETATIONS

Robot kinematics

The structure of the designed robot and its Denavit-Hartenberg description are displayed in Figure 4 and in Table 1, respectively. The first prismatic joint allows the robot to adapt to the patient's vertical position and change the robot configuration according to the surgeon requirements. The next three revolute joints form a spherical wrist whose position reduces the load and the elastic displacements on the robot links. Finally, two revolute joints allow orienting the end-effector while keeping the robot outside of the virtual sphere.

The robot features six DoFs while the kinematic dimension of the neurosurgical task is five, being given by one point and one direction on the space. Therefore the NEUMESY is kinematically redundant. As stated above, the redundancy can be used by the surgeon to choose a suitable robot configuration which minimally interferes with his movements. Indeed, the

Table 1. Denavit-Hartenberg parameters of the NEUMESY

i	$^{i-1}\mathbf{T}_i$	σ_i	α_i	a_i	θ_i	d_i
1	$^{0}\mathbf{T}_1$	1	0	0	0	q_1
2	$^{1}\mathbf{T}_2$	0	$\frac{\pi}{2}$	0	q_2	d_2
3	$^{2}\mathbf{T}_3$	0	$-\frac{\pi}{2}$	0	q_3	0
4	$^{3}\mathbf{T}_4$	0	$\frac{\pi}{2}$	0	q_4	ℓ_2
5	$^{4}\mathbf{T}_5$	0	0	ℓ_3	q_5	0
6	$^{5}\mathbf{T}_6$	0	$\frac{\pi}{2}$	a_6	q_6	0
	$^{6}\mathbf{T}_{tool}$	1	0	0	0	d_t

© copyright FACULTY of ENGINEERING - HUNEDOARA, ROMANIA

origins $O_2 \div O_6$ belong the the same plane on the sheaf (of planes) defined by the LoA. The plane is arbitrary but fixes the robot configuration and the constraints on the surgeon's movements. By choosing a different plane, the space required by the robot for the surgical operation changes and the surgeon's movement could be easier. The solution of the robot inverse kinematic will be presented in the next section.

Solution of the inverse kinematic

For sake of simplicity, let $\mathbf{T}_i$ be the matrix ${}^{i-1}\mathbf{T}_i$, as well as $\mathbf{R}_i = {}^{i-1}\mathbf{R}_i$ the rotation matrix from the frame i to the frame $i-1$ and $\mathbf{p}_i = {}^{i-1}\mathbf{p}_i$ the origin of the frame i referred to the frame $i-1$. The inverse kinematic problem can be expressed as

$$ {}^{0}\mathbf{T}_6 = \breve{\mathbf{T}}^{6}\mathbf{T}_{tool}^{-1} =: \mathbf{T} = \begin{bmatrix} \mathbf{s} & \mathbf{n} & \mathbf{a} & \mathbf{p} \\ 0 & 0 & 0 & 1 \end{bmatrix} \tag{1} $$

where $\breve{\mathbf{T}} = \begin{bmatrix} \breve{\mathbf{s}} & \breve{\mathbf{n}} & \breve{\mathbf{a}} & \breve{\mathbf{p}} \\ 0 & 0 & 0 & 1 \end{bmatrix}$

Equation (1) can be rearranged as

$$ {}^{2}\mathbf{T}_6 = \mathbf{Q}_1 \tag{2} $$

where: ${}^{2}\mathbf{T}_6 = \mathbf{T}_3\mathbf{T}_4\mathbf{T}_5\mathbf{T}_6$ and $\mathbf{Q}_1 = \left({}^{0}\mathbf{T}_2\right)^{-1}\mathbf{T}$

Equation (2) can be rewritten as:

$$ \mathbf{T}_3\mathbf{T}_4\mathbf{T}_5\breve{\mathbf{T}}_6 = \left({}^{0}\mathbf{T}_2\right)^{-1}\mathbf{T}\left(\mathbf{A}_6\right)^{-1} \tag{3} $$

where: $\breve{\mathbf{T}}_6 = \begin{pmatrix} \mathbf{R}_6 & \mathbf{0} \\ \mathbf{0}^T & 1 \end{pmatrix}$ and $\mathbf{A}_6 = \begin{pmatrix} 1 & 0 & 0 & a_6 \\ 0 & 0 & -1 & 0 \\ 0 & 1 & 0 & 0 \\ 0 & 0 & 0 & 1 \end{pmatrix}$

Comparing to each other the left and the right sides of (3), the following equations must hold:

$$ \begin{aligned} \bar{\mathbf{a}} &= \mathbf{R}_3\mathbf{R}_4\mathbf{R}_5\mathbf{R}_6\mathbf{z} \\ \bar{\mathbf{p}} &= \mathbf{R}_3\mathbf{R}_4\mathbf{p}_5 + \mathbf{R}_3\mathbf{p}_4 \end{aligned} \tag{4} $$

where $\bar{\mathbf{a}}$ and $\bar{\mathbf{p}}$ are defined by: $\left({}^{0}\mathbf{T}_2\right)^{-1}\mathbf{T}\left(\mathbf{A}_6\right)^{-1} = \begin{pmatrix} \bar{\mathbf{s}} & \bar{\mathbf{n}} & \bar{\mathbf{a}} & \bar{\mathbf{p}} \\ 0 & 0 & 0 & 1 \end{pmatrix}$ and $\mathbf{z} = [0, 0, 1]^T$. Equations (4) can be further transformed into:

$$ \begin{aligned} \mathbf{R}_4^{-1}\mathbf{R}_3^{-1}\bar{\mathbf{a}} &= \mathbf{R}_5\mathbf{z} \\ \mathbf{R}_4^{-1}\mathbf{R}_3^{-1}\bar{\mathbf{p}} &= \bar{\mathbf{p}}_5 + \mathbf{R}_4^{-1}\bar{\mathbf{p}}_4 \end{aligned} \tag{5} $$

After multiplying left and right sides to each other of the equations (5), it is possible to write:

$$ \bar{\mathbf{p}}\cdot\bar{\mathbf{a}} = \bar{\mathbf{p}}_5\cdot\left(\mathbf{R}_5\mathbf{z}\right) + \left(\mathbf{R}_4^{-1}\bar{\mathbf{p}}_2\right)\cdot\left(\mathbf{R}_5\mathbf{z}\right) \tag{6} $$

where the right side of (6) is zero, since the vectors therein involved are orthogonal. Therefore from (6) the value of the q_1 can be determined, since the projection of $\bar{\mathbf{p}}$ into $\bar{\mathbf{a}}$ depends only on this joint variable. In particular: $q_1 = -\dfrac{d_t\breve{\mathbf{a}}\cdot\breve{\mathbf{n}} + a_6\breve{\mathbf{s}}\cdot\breve{\mathbf{n}} - \breve{\mathbf{p}}\cdot\breve{\mathbf{n}}}{\breve{n}_z} - d_2$ q. When $\breve{n}_z = 0$ the z_0-axis belongs to the operation plane. In this case, if the target point belongs to robot workspace, there are infinite solutions for q_1. Taking into account the module of $\bar{\mathbf{p}}$, there is:

$$ \bar{\mathbf{p}}\cdot\bar{\mathbf{p}} = \mathbf{p}_4\cdot\mathbf{p}_4 + \mathbf{p}_5\cdot\mathbf{p}_5 + 2\left(\mathbf{R}_4\mathbf{p}_5\right)\cdot\mathbf{p}_4 \tag{7} $$

the left side of (7) being noted, since the module of $\bar{\mathbf{p}}$ depends only on joint variable q_1. In this way the value of q_5 can be determined from (7):

$$ \sin q_5 = \frac{\bar{\mathbf{p}}\cdot\bar{\mathbf{p}} - \ell_2^2 - \ell_3^2}{2\ell_2\ell_3} \tag{8} $$

The equation (1) can be rearranged as ${}^{1}\mathbf{T}_5 = \mathbf{Q}_2$, where ${}^{1}\mathbf{T}_5 = \mathbf{T}_2\mathbf{T}_3\mathbf{T}_4\mathbf{T}_5$ and $\mathbf{Q}_2 = \mathbf{T}_1^{-1}\,\mathbf{T}\,\mathbf{T}_6^{-1}$. Considering the new vectors:

$$\begin{aligned}\tilde{\mathbf{s}} &= \mathbf{R}_2\mathbf{R}_3\mathbf{R}_4\mathbf{R}_5\mathbf{x}\\ \tilde{\mathbf{p}} &= \mathbf{R}_2\mathbf{R}_3\mathbf{R}_4\mathbf{p}_4 + \mathbf{R}_2\mathbf{R}_3\mathbf{p}_4 + \mathbf{p}_2\end{aligned} \tag{9}$$

where $\tilde{\mathbf{a}}$ and $\tilde{\mathbf{p}}$ are defined by: $\mathbf{T}_1^{-1}\mathbf{T}\mathbf{T}_6^{-1} = \begin{pmatrix}\tilde{\mathbf{s}} & \tilde{\mathbf{n}} & \tilde{\mathbf{a}} & \tilde{\mathbf{p}}\\ 0 & 0 & 0 & 1\end{pmatrix}$ and $\mathbf{x} = [1, 0, 0]^T$, rearranging (9) as

$$\left(\mathbf{R}_2\mathbf{R}_3\right)^{-1}\tilde{\mathbf{s}} = \mathbf{R}_4\mathbf{R}_5\mathbf{x}$$

$$\left(\mathbf{R}_2\mathbf{R}_3\right)^{-1}\left(\tilde{\mathbf{p}} - \mathbf{p}_2\right) = \mathbf{R}_4\mathbf{p}_5 + \mathbf{p}_4$$

and operating as in (5) it is possible to write:

$$\left(\tilde{\mathbf{p}} - \mathbf{p}_2\right)\cdot\tilde{\mathbf{s}} = \mathbf{p}_5\cdot\left(\mathbf{R}_5\mathbf{x}\right) + \left(\mathbf{R}_4^{-1}\mathbf{p}_4\right)\cdot\left(\mathbf{R}_5\mathbf{x}\right) \tag{10}$$

The left side of (10) depends only on joint variable q_6, while the right side is known, once q_1 and q_5 have been calculated. In this way (10) can be expressed in the form: $\mathrm{Ac}_6 + \mathrm{Bs}_6 = \mathrm{C}$, where

$$A = a_6\breve{\mathbf{s}}\cdot\breve{\mathbf{s}} + d_t\breve{\mathbf{s}}\cdot\breve{\mathbf{a}} - \breve{\mathbf{s}}\cdot\breve{\mathbf{p}} + \breve{s}_z q_1$$

$$B = a_6\breve{\mathbf{s}}\cdot\breve{\mathbf{a}} + d_t\breve{\mathbf{s}}\cdot\breve{\mathbf{s}} - \breve{\mathbf{s}}\cdot\breve{\mathbf{p}} - \breve{a}_z q_1$$

$$C = -(\ell_3 + \ell_2 s_5)$$

The solutions are: $q_6 = \mathrm{atan2}(\pm\sqrt{A^2 + B^2 - C^2}, C) - \mathrm{atan2}(B, A)$.

Equation (1) can be rearranged as: ${}^1\breve{\mathbf{T}}_5 = \mathbf{Q}_3$

where ${}^1\breve{\mathbf{T}}_5 = \mathbf{T}_2\mathbf{T}_3\mathbf{T}_4\breve{\mathbf{T}}_5$, $\mathbf{Q}_3 = \mathbf{T}_1^{-1}\,\mathbf{T}\,\mathbf{T}_6^{-1}\,\mathbf{A}_5^{-1}$, $\breve{\mathbf{T}}_5 = \begin{pmatrix}\mathbf{R}_5 & \mathbf{0}\\ \mathbf{0}^T & 1\end{pmatrix}$ *and* $\mathbf{A}_5 = \begin{pmatrix}\mathbf{I}_3 & \begin{matrix}\ell_3\\ 0\end{matrix}\\ \mathbf{0}^T & \begin{matrix}0\\ 1\end{matrix}\end{pmatrix}$

Considering the vectors:

$$\begin{aligned}\hat{\mathbf{a}} &= \mathbf{R}_2\mathbf{R}_3\mathbf{R}_4\mathbf{R}_5\mathbf{z}\\ \hat{\mathbf{p}} &= \mathbf{R}_2\mathbf{R}_3\mathbf{p}_4 + \mathbf{p}_2\end{aligned} \tag{11}$$

where $\hat{\mathbf{a}}$ and $\hat{\mathbf{p}}$ are defined by $\mathbf{Q}_3 = \begin{pmatrix}\hat{\mathbf{s}} & \hat{\mathbf{n}} & \hat{\mathbf{a}} & \hat{\mathbf{p}}\\ 0 & 0 & 0 & 1\end{pmatrix}$ and rearranging as above, it is possible to write:

$$\mathbf{R}_2^{-1}\hat{\mathbf{a}} = \mathbf{R}_3\mathbf{R}_4\mathbf{R}_5\mathbf{z} \tag{12}$$

$$\mathbf{R}_2^{-1}\left(\hat{\mathbf{p}} - \mathbf{p}_2\right) = \mathbf{R}_3\mathbf{p}_4 \tag{13}$$

From the projection of the equation (13) along $\mathbf{y} = [0, 1, 0]^T$, the value of c_3 can be determined as $c_3 = \dfrac{-d_2 + \hat{p}_z}{\ell_2}$ where $\hat{p}_z = (-\breve{a}_z)d_t + \breve{p}_z - q_1 - \breve{a}_z\ell_3 s_6 - a_6\breve{s}_z - c_6\ell_3\breve{s}_z$

while from the projection of the equation (13) along **z**, it is possible to write $\hat{p}_y c_2 = \hat{p}_x s_2$ where

$$\hat{p}_x = \breve{p}_x - \breve{a}_x(d_t + \ell_3 s_6) - (a_6 + c_6\ell_3)\breve{s}_x$$

$$\hat{p}_y = \breve{p}_y - \breve{a}_y(d_t + \ell_3 s_6) - (a_6 + c_6\ell_3)\breve{s}_y$$

In this way: $q_2 = \mathrm{atan2}(\hat{p}_x, \hat{p}_y) + k\pi$ with $k = 0,1$

Finally, projecting (12) along **z**, the value of c_4 is determined as: $c_4 = \hat{a}_x s_2 - \hat{a}_y c_2$, where $\hat{a}_x = \breve{n}_x$ and $\hat{a}_y = \breve{n}_y$. Therefore: $q_4 = \mathrm{atan2}(c_4, \pm\sqrt{1 - c_4^2})$. There are four solutions for each pose defined by the matrix $\breve{T}$, which mainly differ to each other on the elbow configuration. During the surgical operation only the DAANS is in active mode while the NEUMESY is powered off. Therefore the requirement on the accuracy on the tool positioning concerns only the robot in the static configuration. At the same time, for safety reasons, the contacts between the robot and the virtual sphere have to be avoided.

The link lengths affect both the accuracy and the robot workspace owing to the NEUMESY kinematic structure and have to be appropriately chosen in order to satisfy the requirements stated above. The requirement on the robot workspace can be described by a reachabilty index which gives information about the number of points on the patient's skull being achievable along each desired tool configuration.

© copyright FACULTY of ENGINEERING - HUNEDOARA, ROMANIA

Let the skull surface S be discretized into N points $\mathbf{P}_i$ and the desired tool orientations at $\mathbf{P}_i$ be described by all the vectors $\mathbf{z}_k$ internal to the cone $\Lambda_\alpha(\mathbf{P}_i)$ with vertex at $\mathbf{P}_i$, angle α and axis coincident with the normal to the skull surface in $\mathbf{P}_i$ (Figure 5). Moreover, let the function $\mathrm{IK}(\mathbf{P},\mathbf{z})$ calculate the number of solutions for the inverse kinematic problem:

$$\begin{cases}\mathbf{P}_{tool} = \mathbf{P}\\ \mathbf{z}_{tool} = \mathbf{z}\end{cases}$$

subject to the constraint that all the robot links are external to the virtual sphere. The reachabilty index can be defined as:

$$\Phi_{\ell_2,\ell_3} = \frac{1}{N}\sum_{i=1}^{N}\Theta_\alpha(\mathbf{P}_i), \quad \mathbf{P}_i \in \mathrm{S}$$

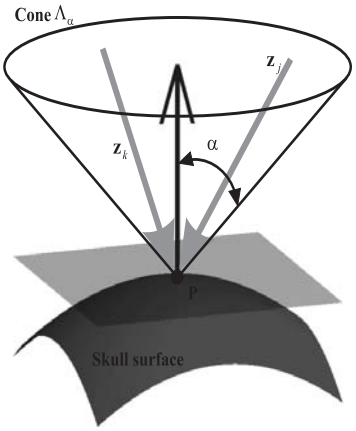

Figure 5. Cone Λ_α

where the function Θ_α returns 1 if, for each vector $\mathbf{z}_k$ belonging to the cone $\Lambda_\alpha(\mathbf{P}_\mathrm{i})$, the function $\mathrm{IK}(\mathbf{P},\mathbf{z})$ is nonzero. The function Θ_α returns 0 otherwise. The index Φ_{ℓ_2,ℓ_3} achieves the maximum (i.e. 1) when every point $\mathbf{P}_i \in \mathrm{S}$ is reachable along any direction internal to its cone $\Lambda_\alpha(\mathbf{P}_\mathrm{i})$.

In order to maximize the robot workspace, the skull surface is taken coincident with the virtual sphere. Therefore the generic point can be described as $\mathbf{P}_i = R\left[\cos\varphi_i\cos\theta_i, \cos\varphi_i\sin\theta_i, \sin\varphi_i\right]^T$ where R is the radius of the virtual sphere and φ_i and θ_i are the polar angles of the point. The angle α is chosen coherently with the tool orientation allowed during a neurosurgical task. A suitable value is $\alpha = 70^\circ$.

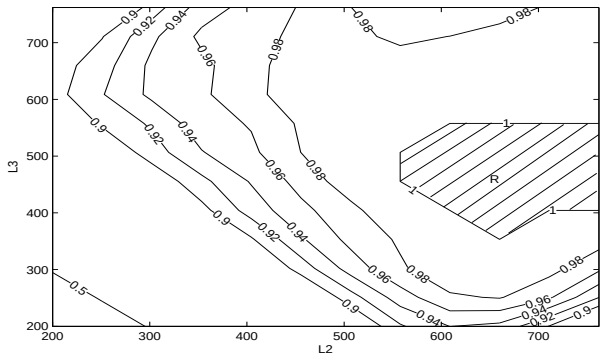

Figure 6: Level curves of Φ_{ℓ_2,ℓ_3} when the robot parameters of Table 2 are assumed

Table 2. Parameters employed in the optimization problem

Parameter	Value
d_2	450 mm
a_6	55 mm
d_t	100 mm
q_1	$\in [0\ , 1200\ \mathrm{mm}]$
$q_i, i = 2..6$	$\in [-170°, +170°]$
α	$\frac{7}{18}\pi$
R	250 mm
$\mathbf{C}$	$[500\ \mathrm{mm},\ 0,\ 800\ \mathrm{mm}]^T$

Figure 6 shows the level curves for Φ_{ℓ_2,ℓ_3} as a function of the link lengths l_2 and l_3 for the robot parameters in Table 2. It can be noticed that the index value is maximum inside the region R, while outside of this region $\Phi_{\ell_2,\ell_3} < 1$, which means that some tool configurations are not reachable by the robot. Since both the index Φ_{ℓ_2,ℓ_3} and the arm stiffness depend on the link lengths, a suitable optimization problem must be defined so as to maximize the robot workspace while keeping the position errors, due to the links deformations, to a minimum.

The optimization problem can be stated as:

$$\begin{aligned}\max_{\ell_2,\ell_3>0} \quad & \frac{1}{\left(\ell_2+\ell_3\right)^3}\\ \text{s.t.} \quad & \Phi_{\ell_2,\ell_3} = 1\\ & \mathbf{P} \in \mathrm{S}\% \qquad \ell_2,\ell_3 > 0\end{aligned}$$

where the cube at the denominator of the objective function takes into account the fact that the link stiffness at the end point is inversely proportional to the cube of link length. With reference to the values of Table 2, the maximum is reached at $\ell_2 = 660\ mm$ and $\ell_3 = 355\ mm$.

In order to highlight the performances of the NEUMESY for the chosen l_2 and l_3 values, let the function Θ_α be modified in $\bar{\Theta}_\alpha(\mathbf{P}_i)$, so that it returns not only a boolean value (0 or 1) but the mean number of solutions for each tool configuration defined by $\mathbf{P}_i \in S$ and $\mathbf{z}_k \in \Lambda_\alpha(\mathbf{P}_i)$:

$$\bar{\Theta}_\alpha(\mathbf{P}_i) = \frac{1}{M} \sum_{\substack{\mathbf{z}_k \in \Lambda_\alpha(\mathbf{P}_i) \\ k=1..M}} \mathrm{IK}(\mathbf{P}_i, \mathbf{z}_k)$$

Figure 7 shows the $\bar{\Theta}_\alpha(\mathbf{P}_i)$ function for the values in Table 2. It can be noticed that there are on average more than ten admissible solutions for each tool configuration.

In order to have a clearer idea of the robot performances, it is convenient to give a spatial representation of the $\bar{\Theta}_\alpha(\mathbf{P}_i)$ index, by introducing a suitable surface $S_{\bar{\Theta}_\alpha}$ defined as:

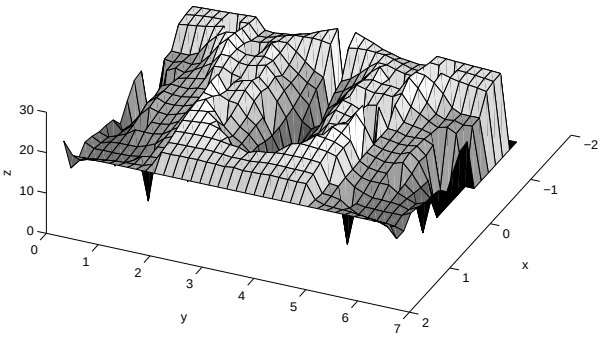

Figure 7. Performance index $\bar{\Theta}_\alpha(\mathbf{P}_i)\}$

$$S_{\bar{\Theta}_\alpha} = \{\mathbf{x} \in \mathbb{R}^3 \mid \mathbf{x} = \frac{1}{R}\bar{\Theta}_\alpha(\mathbf{P})\,\mathbf{P}, \quad \mathbf{P} \in S\}$$

where R is the radius of S.

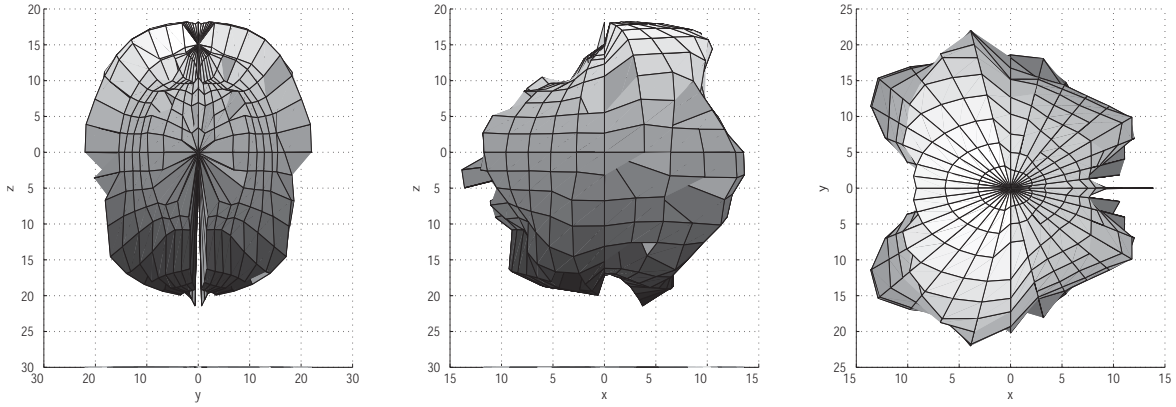

Figure 8. Projections of $S_{\bar{\Theta}_\alpha}$ on the cartesian planes

Figure 8 shows the projections of the $S_{\bar{\Theta}_\alpha}$ on the three principal planes. It can be noticed that the highest performances are achieved on the lateral sides of the virtual sphere, where there is the largest number of configurations allowing the robot to avoid the virtual sphere.

❖ CONCLUSION

In this paper a new robot for neurosurgery is presented. The robot, named NEUMESY, is a six joints serial manipulator designed as positioning device for a neurosurgical actuator previously built by our research group, able to move a low energy x-ray source for the treatment of cerebral lesions. The redundancy respect to the surgical task (5 DoFs, being given by one point and one direction on the space) gives an extra DoF allowing the surgeon to choose the suitable robot configuration which reduces the space required by the robot and maximizes the safety, keeping the robot links away from the patient's head.

The solution of the non-trivial inverse kinematic problem is produced and a kinematic simulator has been carried out in order to analyze the performances of the robot.

Finally, the links length has been optimized in order to satisfy the workspace requirements fixed by the neurosurgical task and reduce the static deformations of the robot arm.

Future works consist in the study of the trajectory planning using the benefits taken by the redundancy so as to limit the link vibrations and deformations during the surgical task.

❖ REFERENCES

[1.] Benabid AL, Cinquin P, Lavalle S, Le Bas JF, Demongeot J, de Rougemont J. Computer-driven robot for stereotactic surgery connected to CT scan and magnetic resonance imaging. Technological design and preliminary results. Appl Neurophysiol 1987; 50:153-154.

© copyright FACULTY of ENGINEERING - HUNEDOARA, ROMANIA

[2.] Benabid AL, Lavallee S, Hoffmann D, Demongeot J, Danel F. Potential use of robots in endoscopic neurosurgery. Acta Neurochir Suppl (Wien) 1992;54:93-97
[3.] Faust R.A. Robotics in Surgery: History, Current and Future Applications. Nova Science Publishers, New York, 2007
[4.] Haidegger T., L. Kovacs, G Fordos, Z. Benyo, P. Kazanzides. Future Trends in Robotic Neurosurgery. Proc. of 14th Nordic-Baltic Conf. on Biomedical Engineering and Medical Physics, 2008
[5.] Haidegger, T. Tian Xia Kazanzides, P. Accuracy improvement of a neurosurgical robot system In Proc. Of BioRob 2008. 2nd IEEE RAS and EMBS Int. Conf. on Biomedical Robotics and Biomechatronics, 19-22 Oct. 2008, 836-841
[6.] Kwoh Y.S., J. Hou, E.A. Jonckheere and S. Hayati A previous termrobotnext term with improved absolute positioning accuracy for CT guided stereotactic brain previous termsurgery. IEEE Trans Biomed Eng 35 (1988), pp. 153-160.
[7.] McBeth P, Deon F. Louw M.D., Peter R. Rizun B.A.Sc.a and Garnette R. Sutherland M.D. Contact Information Robotics in neurosurgery. The American Journal of Surgery, Volume 188, Issue 4, Supplement 1, October 2004, Pages 68-75
[8.] Nathoo N., Cavusoglu MC, Vogelbaum MA, Barnett GH. In touch with robotics: neurosurgery for the future. Neurosurgery. 2005 Mar;56(3):421-33
[9.] Zamorano L, Li Q, Jain S, Kaur G. Robotics in neurosurgery: state of the art and future technological challenges. Int J Med Robot. 2004 Jun;1(1):7-22.
[10.] http://www.mechatronics.it
[11.] http://www.neurochirurgiafirenze.it
[12.] G. Rosati, A. Rossi, and V. Zanotto Lans: a haptic system for minimally invasive radio-surgery *International Journal of Mechanics and Control*, 4(2):45U50, 2003
[13.] A. Rossi, A. Trevisani, and V. Zanotto A telerobotic haptic system for minimally invasive stereotactic neurosurgery *Int. J. Medical Robotics and Computer Assisted Surgery*, Robotic Publications Ltd.,1(2):64-75, 2005
[14.] A.Rossi, A.Gasparetto, A.Trevisani, and V.Zanotto A robotic approach to stereotacticradio-surgery Proc. Of the 7th Biennial *ASME Conference Engineering Systems Design and Analysis*, Manchester, UK, 19-22 July, 2004.
[15.] Duchemin, G. Poignet, P. Dombre, E. Peirrot, F. LIRMM SCALPP: A 6-. dof robot with a non-spherical wrist for surgical applications *Advances in Robot Kinematics*, Kluwer Academic Publisher, 2000, 165-174

ANNALS OF FACULTY ENGINEERING HUNEDOARA
– INTERNATIONAL JOURNAL OF ENGINEERING
copyright © University Politehnica Timisoara,
Faculty of Engineering Hunedoara,
5, Revolutiei, 331128, Hunedoara,
ROMANIA
http://annals.fih.upt.ro